Available online at www.sciencedirect.com
SCIENCE DIRECT®
International Journal of Heat and Mass Transfer 49 (2006) 1176–1184
International Journal of HEAT and MASS TRANSFER
www.elsevier.com/locate/ijhmt

Investigation of moisture transfer effectiveness through a hydrophilic polymer membrane with a field and laboratory emission cell

Li-Zhi Zhang *

Key Laboratory of Enhanced Heat Transfer and Energy Conservation of Education Ministry, School of Chemical and Energy Engineering, South China University of Technology, Wushan Road, Guangzhou 510640, China

Received 1 March 2005; received in revised form 22 July 2005
Available online 25 October 2005

Abstract

This research focuses studies of water permeation potential through a polymer membrane with the help of a standard field and laboratory emission cell. Special efforts are devoted to finding a correlation governing the relations between the number of transfer units (NTU) and the moisture exchange effectiveness. As a first step, moisture diffusivity in the hydrophilic polymer membrane is experimentally measured. In combination with mathematical modeling, the moisture concentration distributions in the cell, the water uptake gradients in the membrane, as well as the local vapor emission rate on membrane surface, are investigated. The results are that the emission rates show a non-uniform character and a polynomial equation governing the moisture exchange effectiveness and the dimensionless number of transfer units, could be used to inversely estimate the diffusivity of water vapor in hydrophilic membranes. The form and the value of constants in the equation are obtained.

Keywords: Moisture transfer; Diffusion; Hydrophilic membranes; Air dehumidification

1. Introduction

Recently, membrane dehumidification processes attracted the attention of the public instead of the other dehumidification processes, such as adsorption, absorption, and refrigeration cycles and so on. From the viewpoint of low cost and low energy requirements, the separation of water vapor from air by membrane separation processes has been studied by many workers [1–5]. Some other workers also studied the membrane systems for total energy recovery [6–8], which has similar mechanisms to air dehumidification.

It is well known that hydrophilic polymer membranes, say, polycellulose acetate, polyvinylidene fluoride, polyethersulfone, Nafion, and polyvinyl alcohol, are useful for the separation of water vapor from other gases in air mixture, because the water molecule is easily incorporated into the hydrophilic polymer membranes, due to the strong affinity between the water molecule and the hydrophilic polymers, which facilitates the transport of water, while impeding the permeation of other gases through the membranes.

Moisture transport properties in such hydrophilic polymer membranes are the most important parameters affecting the system performance and the proper design of the units. Traditionally, the measurements of water vapor diffusivity in membranes are conducted by two ways: transient drying experiments [9–11], and permeation tests [2–4,12]. In the transient drying experiments, transient losses of membrane weight are recorded to calculate the effective moisture diffusivity, with the analytical solution of Fick's second law of diffusion. Though popular and extensively used, this technique has inherent problems: the assumptions and the operating conditions for the analytical solution of Fick's law are very rigorous and any deviation from this would lead to substantial errors [11]. On the other hand, the permeation tests, though directly measure the moisture

* Tel./fax: +86 20 87114268.
E-mail address: Lzzhang@scut.edu.cn

0017-9310/$ - see front matter © 2005 Elsevier Ltd. All rights reserved.
doi:10.1016/j.ijheatmasstransfer.2005.08.029

Nomenclature

C	shape fact or for the isotherm
D_{va}	vapor diffusivity in air (m^2/s)
D_{vm}	moisture diffusivity in membrane (m^2/s)
E_v	local emission rate ($kg\ m^{-2}\ s^{-1}$)
H_d	duct height of air stream (m)
k	convective mass transfer coefficient (m/s)
k_p	partition coefficient (kg air/kg membrane)
N	air exchange rate (s^{-1})
NTU	number of transfer units
r	radius coordinate (m)
Re	Reynolds number
RH	air relative humidity
S	transfer area (m^2)
Sc	Schmidt number
Sh	Sherwood number
T	temperature (K)
t	time (s)
t_r	time to reach steady state (s)
u_a	air bulk velocity (m/s) along radius
V	volume of the cell (m^3)
W_{max}	maximum water uptake of membrane material (kg/kg)
z	coordinates in membrane thickness (m)

Greek symbols

ν	kinematic viscosity of air (m^2/s)
τ	dimensionless time
ω	humidity ratio (kg moisture/kg air)
ε	moisture exchange effectiveness
θ	moisture uptake in membrane (kg moisture/kg dry membrane)
λ	total moisture transfer coefficient ($kg\ m^{-2}\ s^{-1}$)
ρ_a	density of dry air (kg/m^3)
ρ_m	density of membrane (kg/m^3)
δ	membrane thickness (m)

Superscript

*	dimensionless

Subscripts

i	inlet
L	lower chamber
o	outlet
s	surface

transport through membranes at steady state, are rather complicated in the set-up. Most importantly, the obtained data are case-specific, since the convective resistance on both sides of the membrane usually plays an important role in the moisture transport performance, but was always neglected, which would make the results less accurate.

In recent years, field and laboratory emission cell (FLEC) has become the standard equipment for emission test of volatile organic compounds in Europe [13] and some other parts of the world, due to its compactness, high sensitivity, and ease in operation. The author and co-workers have investigated the convective mass transfer characteristics in the cell [14] and measured the emissions of VOCs from dry and wet building materials using the system [15,16]. The fluid dynamics conditions are clear from the previous researches. Studies will be extended to measure the moisture diffusivity through hydrophilic polymer membranes with the system in this work. The NTU-effectiveness relations are also the interests of study, which will provide a guidance in future.

2. Experimental test equipment and procedures

2.1. The FLEC cell

The flow geometry of the FLEC is shown in Fig. 1. It is composed of two parts as shown in Fig. 2: cap (Fig. 2a) and lower chamber (Fig. 2b). When testing, the planar specimen of the emission material is placed in the lower chamber and becomes an integral part of the emission cell. The upper surface of the specimen (the emission surface) and the inner surface of the FLEC cap form a cone-shaped cavity. The air is supplied through the air slits in the cap. It is introduced through two diametrically positioned inlets (symmetrically placed) into a circular-shaped channel at the perimeter, from where the air is distributed over the emission surface through the circular air slit. The air flows inward radially, until it exits the FLEC outlet in the center.

2.2. The whole set-up

In this test, saturated NaCl solution is poured into the lower chamber of the FLEC cell. Then a hydrophilic polymer membrane is covered on the lower chamber. Following this step, the cap of the FLEC is placed on the membrane to form a sandwiched structure. The membrane holding module is shown in Fig. 3. A 1 mm gap between the sodium chloride solution and the membrane tested is kept. The saturated solution in the lower chamber supplies a constant humidity ratio below the membrane lower surface. When the humidity ratio between the two sides of the membrane is different, moisture will diffusive through the membrane. Humid air is supplied from the inlets of the cap, which will exchange moisture with the membrane and the humidity ratio will change along the path. During the test, the temperature is kept constant. The relative humidity of the inlet and the outlet air streams are measured, and the moisture exchange effectiveness can be calculated.

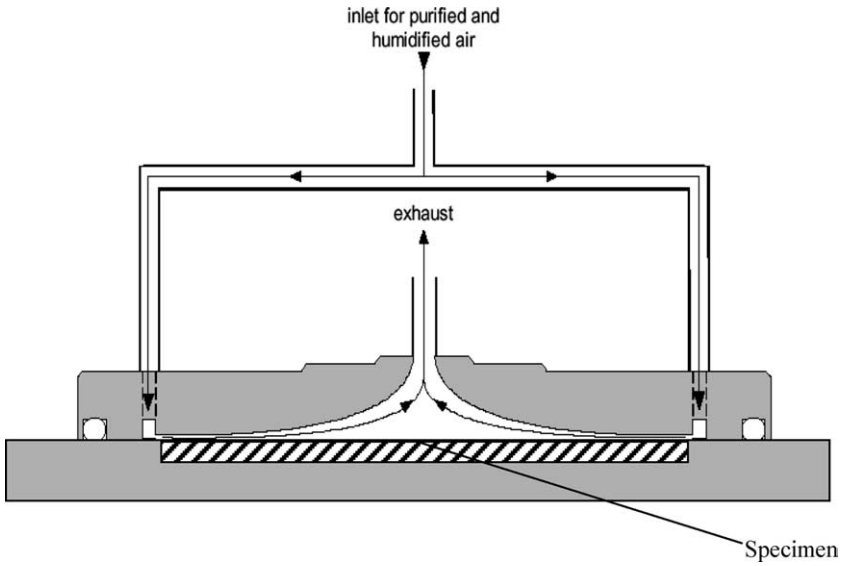

Fig. 1. A schematic showing the flow geometry of the FLEC.

The cell is supplied with clean and humidified air from an auxiliary air supply unit of FLEC. The complete test rig is shown in Fig. 4. The supply air flows from a compressed air bottle and is purified through an AC carbon column filter and is then split into two streams. One of them is humidified through a bubbler immersed in a bottle of distilled water, and then re-mixed with the other dry air stream. The outlet humidity from the bottle with bubbler reaches nearly 100%. The humidity of the mixed air stream is controlled by adjusting the ratios of air mixing by two needle valves on each stream. The desired relative humidity is obtained with this method. The airflow rates are controlled by two air pumps/controllers at the inlet and outlet of the FLEC. This kind of pump has a built-in PID controller which keeps the flow rates to the set points. To prevent outside air from infiltrating into the FLEC, a manometer is installed to monitor the pressure inside the FLEC and ensure that it is positive. The humidities to and from the FLEC cell are measured by RH sensors, which are installed after the pumps/controllers. The measuring accuracies are, respectively, 2% for relative humidity, and 2.5% for airflow rate. The total uncertainty is less than 7.5%. The design of the system allowed versatility of membrane replacement and the use of existing knowledge of flow in the cell.

2.3. Experimental procedure

Before each test, the humidity sensors and the flow meters are carefully calibrated with a chilled-mirror dew point meter (accuracy 0.1 °C) and a floating ball flow meter (10 ml/min), respectively. Then the saturated NaCl solution is poured into the lower chamber. Additional NaCl crystals are added to the solution to ensure the solution saturated. Following this step, the tested membrane is placed on the lower chamber and a sandwiched structure is formed with the cap placed on the membrane. Special care is taken to prevent the membrane be wetted by the solution. Then the FLEC cell's outlet and inlet are closed for 24 h to let the membrane and the cell volume become fully equilibrium with the NaCl solution.

The membrane used is a commercially available hydrophilic mixed cellulose membrane supplied by a local company. This material is cheap and strong mechanically. The physical properties are pre-determined in the laboratory. They are: pore size, 0.1 μm; porosity, 0.76; membrane thickness, 100 μm; maximum moisture uptake, 0.35; isotherm shape factor, 0.86; density, 760 kg/m^3.

After the 24 h equilibrium stage, the supply air is adjusted through the controlling valves to the desired flow rate and the desired relative humidity. Then the valves before and after the FLEC cell are opened to let the conditioned air stream flow through the cell. In the cell, the air stream exchanges moisture with the membrane, and consequently exits the system. Relative humidities are recorded by a data logging system as the air stream begins to flow the cell. This process continues for 2–3 h, long after the moisture transfer becomes fully steady and the outlet relative humidity reaches a stable value. The whole test is performed under room temperature conditions and it is controlled to within 0.5 °C variations during the test. Constant inlet relative humidity and air flow rates are maintained by the air supply unit.

After each test, the inlet humidity and air flow rates are set to new values to perform the next experiment. Modifications to the air supply unit are done to supply larger volumetric flow rates than the original FLEC system can.

3. Model development

The governing equations for predicting the moisture transport in the emission cell are developed. The schematic

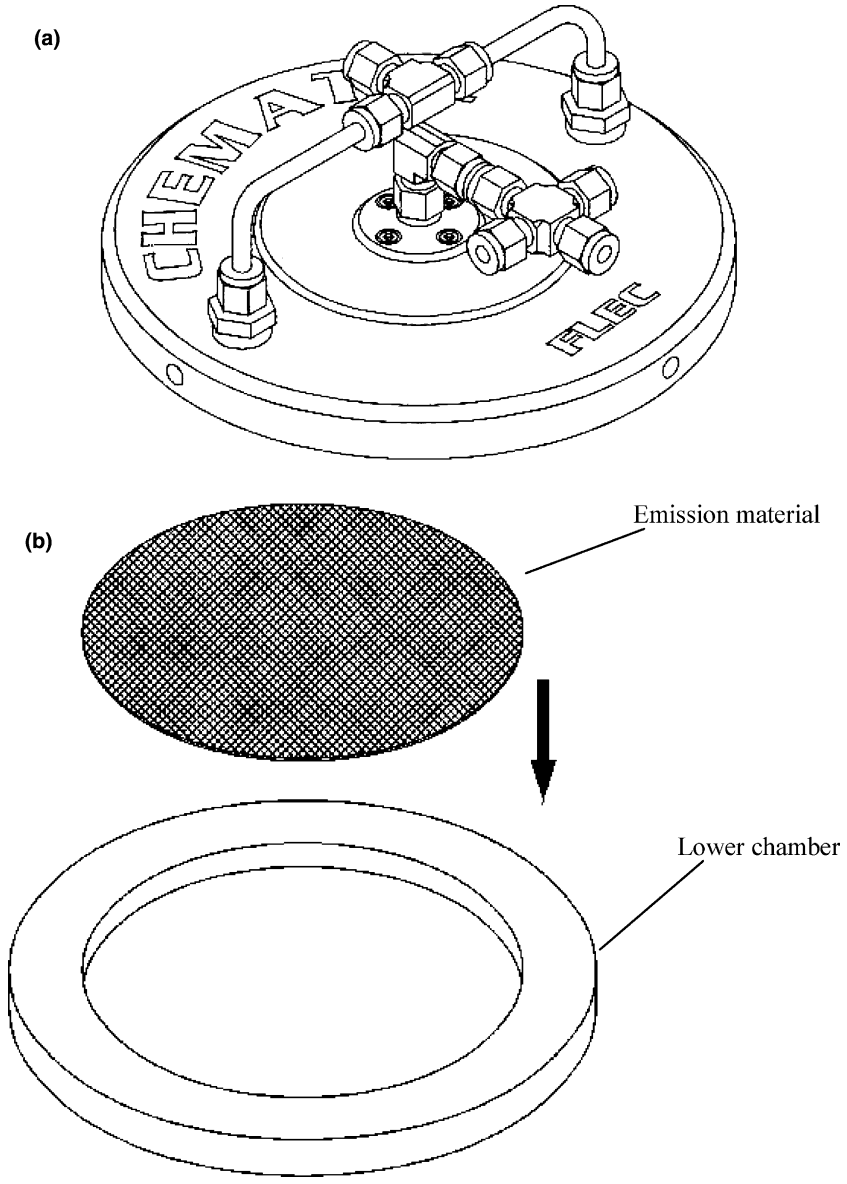

Fig. 2. A view of the FLEC, showing the cap (a) and lower cavity (b).

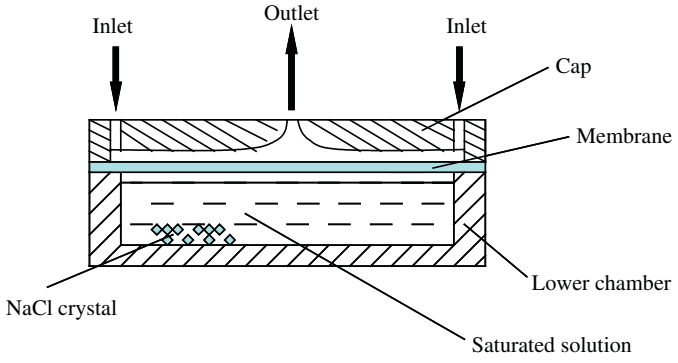

Fig. 3. Arrangement of FLEC Cell with tested membrane and NaCl solution.

of the problem is represented in Fig. 5. A control volume based mass balance method is employed to obtain the partial differential equations. To aid in the analysis, some assumptions are made as following:

(1) Fick's law applies to the moisture diffusion in membrane. The thermo-physical properties of membrane keep constant throughout the experiment. The process is isothermal.
(2) Moisture diffusion in the flow direction in the air stream is negligible compared to vapor convection by bulk flow. This assumption is true for Peclet number greater than 10.
(3) Vapor diffusion in membrane is one-dimensional and in thickness direction. This is valid considering the large dimensional differences in membrane geometry.
(4) The saturated solution is in equilibrium with membrane lower surface throughout the test process.

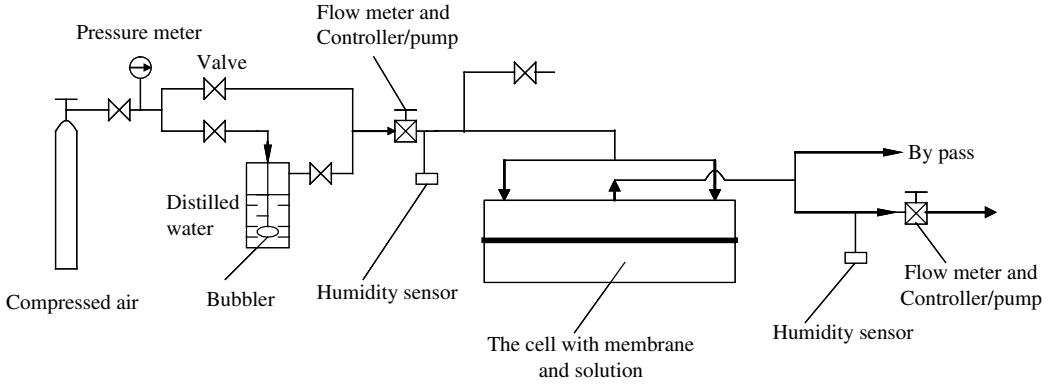

Fig. 4. Experimental equipment set-up for moisture transport tests.

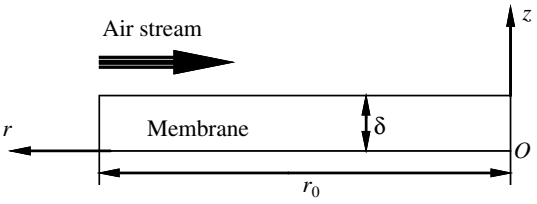

Fig. 5. A schematic of the problem.

The moisture conservation in air stream gives:

$$\frac{\partial \omega}{\partial t} + u_a \frac{\partial \omega}{\partial r} = \frac{E_v}{H_d \rho_a} \tag{1}$$

where ω is the humidity ratio (kg moisture/kg air); t is time (s); u_a is air bulk velocity (m/s) along radius; r is radius coordinate (m); E_v is the local emission rate from the membrane to air (kg m^{-2} s^{-1}); H_d is duct height of air stream (m); ρ_a is density of dry air (kg/m^3). FLEC cell is specially designed that a constant u_a along the radius is realized.

Moisture diffusion in membrane

$$\frac{\partial \theta}{\partial t} = \frac{\partial}{\partial z}\left(D_{vm} \frac{\partial \theta}{\partial z}\right) \tag{2}$$

where θ is moisture uptake in membrane (kg moisture/kg dry membrane); z is coordinates in membrane thickness (m); D_{vm} is moisture diffusivity in membrane (m^2/s).

Local moisture emission rate

$$E_v = -\rho_m D_{vm} \left.\frac{\partial \theta}{\partial z}\right|_{z=\delta} \tag{3}$$

where ρ_m is density of membrane (kg/m^3).

The relation between the moisture uptake and air humidity is summarized by an isotherm curve as

$$\theta = \frac{W_{max}}{1 - C + C/\mathrm{RH}} \tag{4}$$

where W_{max} is the maximum water uptake of membrane material (kg/kg); C is a constant named the shape factor for the material; RH is air relative humidity.

The relative humidity is calculated by humidity ratio and temperature as [17]

$$\frac{\mathrm{RH}}{\omega} = \frac{e^{5294/T}}{10^6} - 1.61\mathrm{RH} \tag{5}$$

where T is in K. The second term on the right side of the equation will generally have less than a 5% effect, and it can be usually neglected.

Initial conditions:

$$t = 0, \quad \omega = \omega_L, \quad \theta = \theta_L \tag{6}$$

where ω_L is the humidity ratio determined by the saturated NaCl solution and temperature (kg/kg); and θ_L is the water uptake of membrane in equilibrium with the solution vapor.

Boundary conditions for air stream:

$$r = r_0, \quad \omega = \omega_i \tag{7}$$

$$r = 0, \quad \text{outflow} \tag{8}$$

Boundary conditions for membrane:

$$z = \delta, \quad \omega = \omega_s \tag{9}$$

$$z = 0, \quad \omega = \omega_L \tag{10}$$

where ω_i is the set point of humidity ratio of inlet air, ω_s is the humidity ratio on membrane surface. The relations between the humidity ratio on surface and in air stream are

$$k\rho_a(\omega_s - \omega) = -\rho_m D_{vm} \left.\frac{\partial \theta}{\partial z}\right|_{z=\delta} \tag{11}$$

where k is the convective mass transfer coefficient (m/s).

The convective mass transfer coefficients are related to the fluid dynamics in the cell, which are studied in detail in a previous research [14]. Figs. 6 and 7 show the streamlines and the velocity vectors in the cell (cap above the membrane surface) from CFD simulations. A correlation has also been obtained to calculate this property [14] as

$$Sh = 0.3359 Re\, Sc \left(\frac{r_0 - r}{2H_d}\right)^{-0.834} \tag{12}$$

where Sh, Re, and Sc are Sherwood number, Reynolds number and Schmidt number, respectively. They are defined as

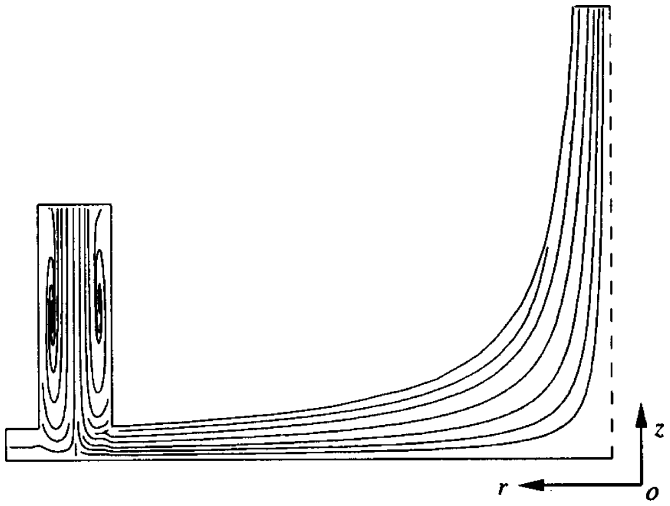

Fig. 6. Streamlines representation in a cross-section of the chamber above membrane.

$$Sh = \frac{2kH_d}{D_{va}} \tag{13}$$

$$Re = \frac{2u_a H_d}{v} \tag{14}$$

$$Sc = \frac{v}{D_{va}} \tag{15}$$

where D_{va} is the vapor diffusivity in air (m^2/s); v is the kinematic viscosity of air (m^2/s). Water uptake and humidity ratio on membrane surface satisfies the isotherm equation of Eq. (4).

If Henry's sorption law applies to the membrane material

$$\theta = k_p \omega \tag{16}$$

where k_p is the partition coefficient, kg air/kg membrane.

Re-arrangement of Eq. (11) and substituting it into Eq. (3) gives

$$E_v = \frac{\omega_L - \omega}{\frac{1}{k\rho_a} + \frac{\delta}{D_{vm}\rho_m k_p}} \tag{17}$$

We define the total moisture transfer coefficient as

$$\lambda = \frac{1}{\frac{1}{k\rho_a} + \frac{\delta}{D_{vm}\rho_m k_p}} \tag{18}$$

Then the number of transfer units is defined by

$$\mathrm{NTU} = \frac{\lambda S}{NV\rho_a} \tag{19}$$

where S is the transfer area of the membrane surface (m^2); N is the air exchange rate (s^{-1}); V is the volume of the cell (m^3).

4. Results and discussion

4.1. Estimation of moisture diffusivity

The transient equations for air stream, membrane and air-membrane interface are solved in a coupled way with finite difference techniques. Iterations are necessary to find a converged solution. At each time step, mass balances between the air stream, the membrane, and the air/membrane interface are ensured. The outlet air relative humidity can be calculated with moisture distributions in the cell and the local moisture emission rates on the membrane. The outlet RH first decreases and then reaches a stable value, indicating that moisture transport becomes stable. This stable value is called the steady state outlet relative humidity. Fig. 8 plots the curve of various steady state outlet RH with various assumed diffusivities under operating conditions of 5 L/min, 10% RH inlet air.

The true value of membrane diffusivity is at the point where the measured RH intersects with the response curve. In this case, as shown in Fig. 8, the measured diffusivity for the mixed cellulose membrane should be 3.6×10^{-10} m^2/s.

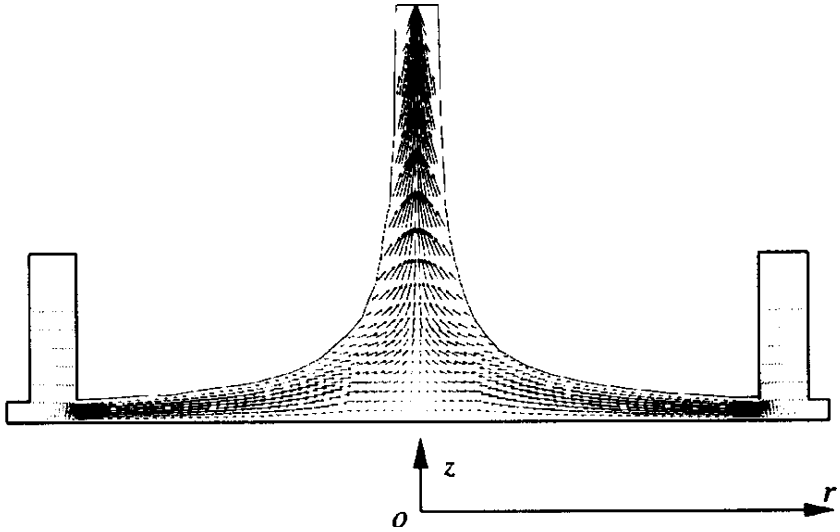

Fig. 7. Velocity vectors in the cross-section crossing air inlets tubes in the chamber.

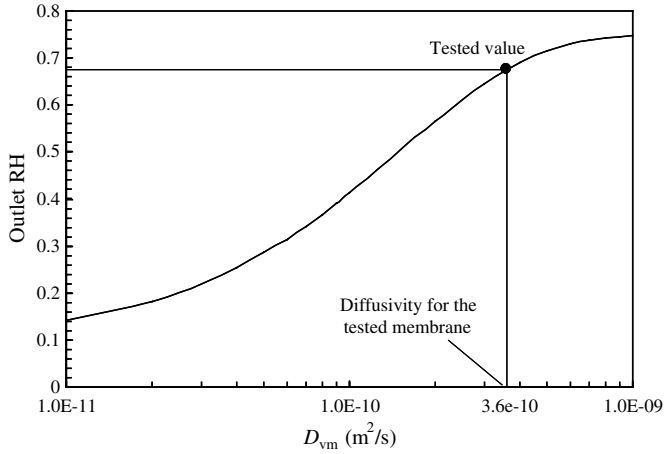

Fig. 8. Response curve of the outlet relative humidity and the tested data for the mixed cellulose membrane. Inlet air, 5 L/min at 10% RH.

The benefits with this method are that it simultaneously considers the cell fluid dynamics, membrane configurations and operating conditions.

To validate the model, the transient lapses of outlet RH with time for different flow rates are depicted in Fig. 9. The discrete dots are the measured values. As can be seen from the figure, the model predicts the tested data reasonably well. Generally it takes 1–2 min for the moisture transport becomes steady. After this transient period, stable transport of moisture from the solution to the air stream is established. The greater the air flow rates, the less the outlet RH. When the air flow rates are less than 5 L/min, no obvious humidity change observed for air stream flowing through the cell, and the outlet air becomes saturated with the solution. The transient responses of outlet RH are mainly influenced by the initial conditions: moisture in the cell volume, and in the membrane. At the beginning, air mainly drives out the initial moisture in the chamber and in the membrane that was stored before the test, outlet humidity is relatively high. With time going, initial moisture in cell and membrane is exhausted out step by step, and the outlet humidity comes to a steady value, which is solely determined by permeation through membrane.

4.2. Moisture transport in the cell

Using the proposed model, the moisture distribution in the cell can be investigated. The operating conditions in the following are that air flow rates: 10 L/min; inlet humidity, 20%; temperature 16 °C. Fig. 10 shows the variations of local relative humidity of the air stream along radius coordinates at different time. Dimensionless time τ is defined as

$$\tau = \frac{t}{t_r} \tag{20}$$

where t_r is the time when outlet humidity reaches 99.0% of its steady state value.

As seen from this figure, air humidity rises continuously from inlet to outlet, indicating continuous moisture emissions from the membrane to air stream. Locally, air humidity also rises, fast in the beginning and slowly subsequently, with time in the transitional period.

The local emission rates along the membrane radius are plotted in Fig. 11. From inlet to outlet, the moisture emission rates decrease, almost linearly, along the membrane radius. At the beginning, emission rates near the inlet are much higher, and those near the outlet are lower. With time going, the emission rates near the inlet drop somewhat, while the emission rates near the outlet rise by a certain amount. In other words, when the moisture permeation is transiting from transient state to steady state, the slop of emission becomes less steep.

To deeply disclose the distributed character of the emission rates, the water uptake contours in the membrane are drawn in Fig. 12 for the steady state transfer period. The dimensionless thickness coordinates are defined as

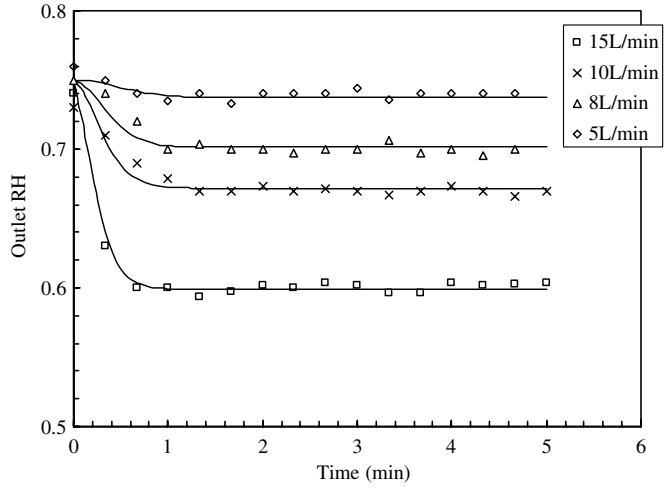

Fig. 9. Variations of the outlet RH with lapse of time for different flow rates with the membrane. The discrete dots are experimental data and the solid lines are calculated with the model.

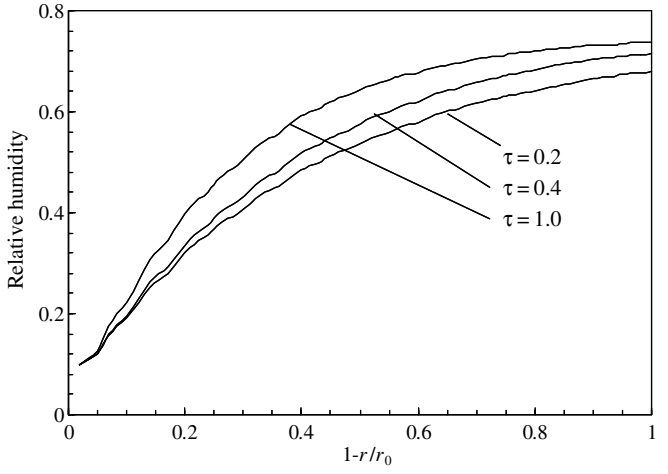

Fig. 10. The distribution of relative humidity of the air stream above the membrane, along the cell radius at different time.

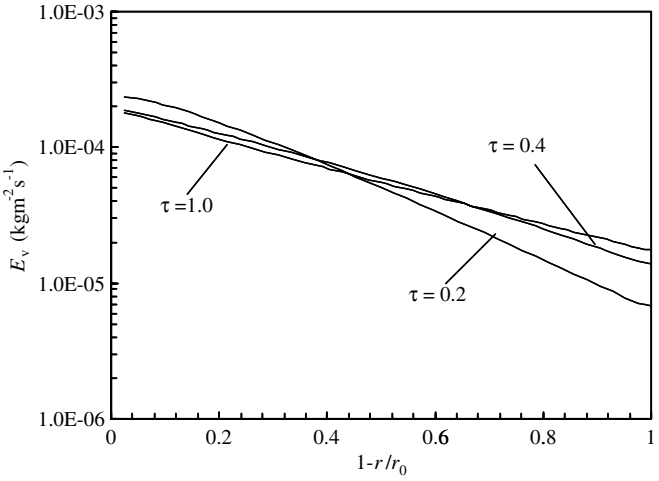

Fig. 11. Variations of local emission rate on membrane surface along membrane radius at different time.

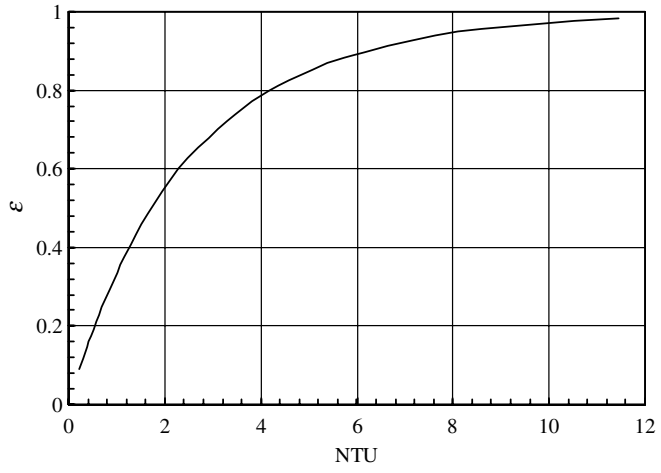

Fig. 13. The variations of the moisture exchange effectiveness with the number of transfer units.

$$z^* = \frac{z}{\delta} \tag{21}$$

From this figure, the two-dimensional water uptake fields are clear. The water uptake is the largest in the right-down corner, but the least in the up-left corner. This distribution of water uptake is in accordance with the variations of moisture emission rates on membrane surface. Near the air inlet, uptake gradients are higher, and more moisture is driven through the membrane; while near the outlet, uptake gradients are lower, and less moisture can be driven through the membrane. The model proposed takes into account the disparities of moisture transfer on different membrane surfaces.

4.3. NTU-effectiveness curve

Similar to the analysis of a heat exchanger, a moisture exchange effectiveness can be defined as

$$\varepsilon = \frac{\omega_o - \omega_i}{\omega_L - \omega_i} \tag{22}$$

where subscripts o, i, refer to air outlet and inlet respectively, ad L to solution humidity in lower chamber. Fig. 13 plots the calculated moisture exchange effectiveness from the distributed model with various number of transfer units. When the NTU is from 0 to 6, ε rises sharply with NTU. When the NTU is greater than 6, there's little merit in further increasing ε by an increase of NTU. When the membrane thermo-physical properties and the experimental conditions are known, NTU can be calculated from this curve with the measured moisture exchange effectiveness. Finally, the diffusivity can be obtained.

A polynomial correlation can be fitted to represent this curve as

$$\varepsilon = -0.0002\mathrm{NTU}^4 + 0.0052\mathrm{NTU}^3 - 0.0638\mathrm{NTU}^2 + 0.3759\mathrm{NTU} + 0.015 \tag{23}$$

$$R_2 = 0.9998 \tag{24}$$

This correlation applies to the FLEC system with membrane diffusion.

5. Conclusions

How to estimate vapor diffusivity in membranes is one of the most important issues in membrane related technology. In this work, a standard filed and laboratory emission cell has been used to predict the moisture diffusivity in hydrophilic polymer membranes. The membrane thermo-physical properties and the hydrodynamics in the cell geometry are considered simultaneously. Based on this step, the NTU-effectiveness method is then used to study the moisture transport characteristics in the unit.

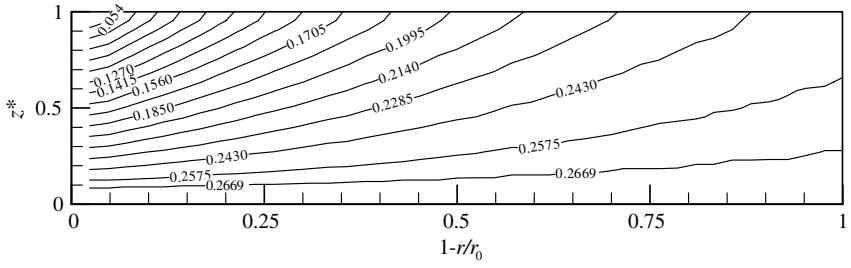

Fig. 12. Contours of water uptake in membrane at steady state.

With the model proposed in the study, distributions of air humidity and emission rates on membrane surface demonstrate a non-uniform character. The tested membrane's diffusivity can be estimated from the response curve of outlet RH. For the mixed cellulose membrane, the measured diffusivity is 3.6×10^{-10} m^2/s. The water permeation potential can be reflected by an effectiveness-number of transfer units curve. A correlation has been obtained to summarize this relation.

Acknowledgement

This Project 50306005 is supported by National Natural Science Foundation of China.

References

[1] V. Morillon, F. Debeaufort, G. Blond, A. Voilley, Temperature influence on moisture transfer through synthetic films, J. Membr. Sci. 168 (2000) 223–233.
[2] X.H. Ye, M.D. Levan, Water transport properties of Nafion membranes. Part I. Single-tube membrane module for air drying, J. Membr. Sci. 221 (2003) 147–161.
[3] P. Scovazzo, J. Burgos, A. Hoehn, P. Todd, Hydrophilic membrane based humidity control, J. Membr. Sci. 149 (1998) 69–81.
[4] P. Scovazzo, A. Hoehn, P. Todd, Membrane porosity and hydrophilic membrane based dehumidification performance, J. Membr. Sci. 167 (2000) 217–225.
[5] K.L Wang, S.H. Mccray, D.D. Newbold, E.L. Cusseler, Hollow fiber air drying, J. Membr. Sci. 72 (1992) 231–244.
[6] K.R. Kistler, E.L. Cussler, Membrane modules for building ventilation, Chem. Eng. Res. Des. 80 (2002) 53–64.
[7] L.Z. Zhang, Y. Jiang, Heat and mass transfer in a membrane-based energy recovery ventilator, J. Membr. Sci. 163 (1999) 29–38.
[8] L.Z. Zhang, J.L. Niu, Effectiveness correlations for heat and moisture transfer processes in an enthalpy exchanger with membrane cores, ASME J. Heat Transfer 122 (5) (2002) 922–929.
[9] G.K. Vagenas, V.T. Karathanos, Prediction of the effective moisture diffusivity in gelatinized food systems, J. Food Eng. 18 (1993) 159–179.
[10] S.U. Hong, J.L. Duda, Diffusion of CFC11 and hydrofluorocarbons in polyurethane, J. Appl. Polym. Sci. 70 (1998) 2069–2073.
[11] P. Hernandez-Munoz, R. Gavara, R.J. Hernandez, Evaluation of solubility and diffusion coefficients in polymer film-vapor systems by sorption experiments, J. Membr. Sci. 154 (1999) 195–204.
[12] H. Okuno, K. Renzo, T. Uragami, Sorption and permeation of water and ethanol vapors in polyvinylchloride membrane, J. Membr. Sci. 103 (1995) 31–38.
[13] CEC—Commission of the European Communities, prENV 13419-2, Building Products—Determination of the Emission of Volatile Organic Compounds—Part 2: Emission Test Cell Method, European Committee for Standardization, Brussels, 1998.
[14] L.Z. Zhang, J.L. Niu, Laminar fluid flow and mass transfer in a standard field and laboratory emission cell (FLEC), Int. J. Heat Mass Transfer 46 (2003) 91–100.
[15] L.Z. Zhang, J.L. Niu, Modeling VOCs emissions in a room with a single-zone multi-component multi-layer technique, Build. Environ. 39 (2004) 523–531.
[16] L.Z. Zhang, J.L. Niu, Mass transfer of volatile organic compounds from painting material in a standard field and laboratory emission cell (FLEC), Int. J. Heat Mass Transfer 43 (2003) 2415–2423.
[17] C.J. Simonson, R.W. Besant, Energy wheel effectiveness. Part I—development of dimensionless groups, Int. J. Heat Mass Transfer 42 (1999) 2161–2170.